ELSEVIER

Journal of Power Sources 97–98 (2001) 412–414

JOURNAL OF POWER SOURCES

www.elsevier.com/locate/jpowsour

In situ XAFS study of the electrochemical deintercalation of Li from $Li_{1-x}Mn_{2-y}Cr_yO_4$ ($y = 1/9, 1/6, 1/3$)

Izumi Nakai[a,*], Kenji Yasaka[a], Hiroshi Sasaki[a], Yasuko Terada[a], Hiromasa Ikuta[b], Masataka Wakihara[b]

[a]*Department of Applied Chemistry, Faculty of Science, Science University of Tokyo, Kagurazaka, Shinjuku, Tokyo 162-8601, Japan*
[b]*Department of Chemical Engineering, Tokyo Institute of Technology, Ookayama, Meguro-ku, Tokyo 152, Japan*

Received 28 June 2000; received in revised form 29 January 2001; accepted 4 February 2001

Abstract

Chemical states and structural changes accompanying the electrochemical Li deintercalation of $Li_{1-x}Mn_{2-y}Cr_yO_4$ ($y = 1/9, 1/6, 1/3$) were studied by the in situ X-ray absorption fine structure (XAFS) technique. The X-ray absorption near-edge structures (XANES) of Mn and Cr as a function of x showed that the 4 V plateau of the material can be ascribed to the oxidation of Mn^{3+} to Mn^{4+}, and Cr does not contribute to the charging, but to the stabilization of the spinel structure against the delithiation. The extended EXAFS analysis of $Li_{1-x}(Mn, Cr)_2O_4$ revealed that the Jahn–Teller distorted Mn^{3+}–O octahedra become uniform when the cell is fully charged.

Keywords: In situ XAFS; Jahn–Teller distortion; Spinel; Cathode material; Chromium substitution

1. Introduction

Spinel compounds attract much attention as the most promising cathode material for 4 V lithium ion batteries. However, one problem with stoichiometric $LiMn_2O_4$ is that it exhibits capacity fading upon cycling [1–3]. It is reported that the cyclic performance of $LiMn_2O_4$ is improved by a partial substitution of Mn by Cr, Co or Ni [4,5]. Wakihara et al. showed that the improvement of the cycle performance is caused by the enhancement of the stability of octahedral sites in the spinel skeleton structure [5–8]. They found that the diffusion coefficient of lithium in $Li(Mn_{2-y}Cr_y)O_4$ increased with the increase of the amount of chromium (y). This increase could be explained by considering the changes in metal–oxygen bonding in the spinel structure, i.e. stabilization of the MO_6 octahedra causes smooth diffusion of lithium in the 8a–16c–8a diffusion path. In order to prove this hypothesis, we have conducted X-ray spectroscopic analyses of these materials.

Powder diffraction techniques only offer limited structural information on long-range-order. In contrast, the X-ray absorption fine structure (XAFS) technique provides independent information as to the chemical state and local structure of the chromium atom, as well as that of the host manganese atoms. Ammundsen et al. [9,10] reported that the oxidation states of the chromium in the initial stage is Cr^{3+} (from XAFS). They also reported in detail the effect of chemical extraction and sorption of lithium in HCl and LiOH on the structure of spinel. However, the oxidation mechanisms of the manganese and chromium in electrochemical Li deintercalation remains to be elucidated. We have developed an in situ transmission XAFS cell [11] to analyze the electrochemical reaction in rechargeable Li battery materials. The Li deintercalation behavior of $LiNiO_2$, $LiCoO_2$, $Li(Ni, Co)O_2$, and $LiMn_2O_4$ has been clarified by our XAFS technique [12–15]. This method allows us to obtain XAFS data of the electrode materials at any deintercalation–intercalation stage without disassembling the cell.

The present study was conducted to reveal by in situ XAFS analysis variations in the chemical states and the local structure of the manganese and chromium in $Li_{1-x}(Mn, Cr)_2O_4$ as a function of the lithium content.

2. Experimental

The chromium substituted manganese spinels $Li(Mn_{2-y}Cr_y)O_4$ were prepared by reacting a stoichiometric

* Corresponding author. Tel.: +81-3-3260-3662; fax: +81-3-3235-2214.
E-mail address: inakai@ch.kagu.sut.ac.jp (I. Nakai).

0378-7753/01/$ – see front matter
PII: S0378-7753(01)00742-X

mixture of Li_2CO_3 (99%, Wako Pure Chemical Industries Ltd.) and $Mn(CH_3COOH)_2{\cdot}4H_2O$ (99%, Wako Pure Chemical Industries Ltd.) by adding Cr_2O_3 (reagent grade, Yoneyama Chemical Industries Ltd.). The mixture was preheated at 600°C for 6 h, then heated at 750°C for 3 days in air. The products were identified by X-ray powder diffraction method. The in situ XAFS cells incorporated a thin-film cathode, a liquid electrolyte (1 M $LiBF_4$ in PC + EC), and a lithium-foil anode. Details of the cell were described in our previous paper [11]. Manganese and chromium K-XAFS spectra were measured by the transmission mode at various stages of the charge process. The measurements were carried out using synchrotron radiation at BL-7C, Photon Factory, High Energy Accelerator Research Organization, Tsukuba, Japan. The cell was charged to a desired voltage at a constant current; it was then kept in a resting condition for ca. 40 min. The EXAFS data were analyzed by conventional methods using REX2 data analysis software [16]. Theoretical parameters used in the curve fitting analysis were calculated by FEFF8 [17].

3. Results and discussion

The Mn and Cr K-XANES spectra for $Li_{1-x}Mn_{5/3}Cr_{1/3}O_4$ measured as a function of x are shown in Fig. 1(a) and (b), respectively. The Mn K-edge absorption energy shifts to higher energies with increasing x, while the Cr K-edge shows no significant shift. This indicates that Mn^{3+} is oxidized to Mn^{4+} with the electrochemical lithium deintercalation, while chromium remains its original trivalent state even after the delithiation. A similar tendency was reported for chemical extraction of lithium [9,10].

To compare the effect of the amount of chromium substitution for manganese, XANES spectra for $Li(Mn_{2-y}Cr_y)O_4$ for $y = 0$, 1/9, 1/6, and 1/3 were compared. The positive shift of the Mn K-edge is smallest for $Li(Mn_{2-y}Cr_y)O_4$, $y = 0$ and largest for $y = 1/3$. This result is reasonable considering that the nominal oxidation state of manganese in these materials increase from 3.5 ($y = 0$) to 3.6 ($y = 1/3$). The 1s to 3d transition of the transition metal is formally forbidden on the basis of dipole selection rules if the octahedral oxygen coordination around the metal atom has O_h symmetry. The lowering of the symmetry partially allows the transition and causes the appearance of the so-called pre-edge peak on the lower energy side of the main K-absorption edge. This pre-edge absorption is also sensitive to the electronic state of the absorber atom. Fig. 2 shows the variation of the pre-edge absorption of Mn K-edge as a function of x for different chromium content (y). The pre-edge peak in Fig. 2 is apparently made up of two components, which can be ascribed to Mn^{3+} and Mn^{4+} as designated in the figures. The electrochemical deintercalation of lithium causes an increase in the intensity of the Mn^{4+} peak, which further supports the oxidation of manganese with the lithium deintercalation. The effect of chromium content on the pre-edge peak is not observed clearly in these three materials due to the small differences in y.

Fourier transforms (FT) of the EXAFS oscillations yields a pseudo-radial distribution function of the local atomic

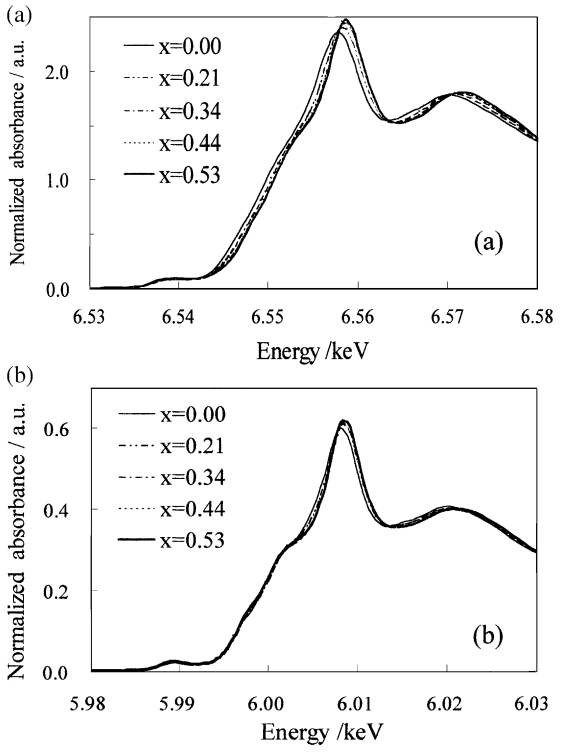

Fig. 1. (a) Mn and (b) Cr K-XANES spectra for $Li_{1-x}Mn_{5/3}Cr_{1/3}O_4$ as a function of Li deintercalation (x).

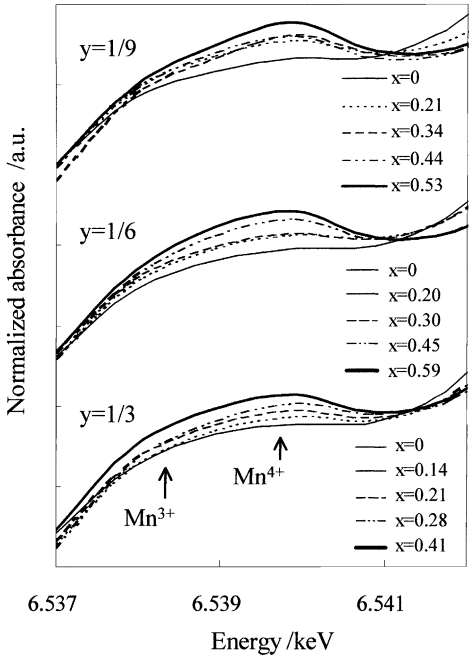

Fig. 2. Variations of the pre-edge peak for $Li_{1-x}Mn_{2-y}Cr_yO_4$ for different x and y (Mn K-edge).

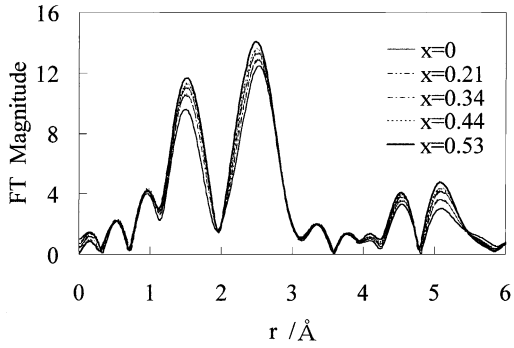

Fig. 3. Variations in the Fourier transforms (FT) of the Mn K-edge EXAFS for $Li_{1-x}Mn_{5/3}Cr_{1/3}O_4$ as a function of Li deintercalation (x).

environment around the absorber atom. FT of the k^3-weighted Mn K-edge EXAFS oscillation of $Li(Mn_{2-y}Cr_y)O_4$ with $y = 0$, 1/9, 1/6, and1/3 were calculated. Fig. 3 shows the results for $y = 1/3$. The abscissa is the distance from the central manganese absorber atom, and is not corrected for the phase shift. The first peak at around 1.5 Å corresponds to the Mn–O interaction in the first coordination sphere; the second peak at around 2.5 Å is a contribution largely from the Mn–Mn interaction in the second coordination sphere, where the Mn–Li interaction is negligible because of the low back-scattering power of the lithium. The peak at around 4.5 Å represents the second Mn–Mn interaction, and the peak at around 5.2 Å is derived from the linear single-scattering and the multi-scattering caused by the manganese atoms at twice the distance of the nearest manganese. As can be seen from Fig. 3, the electrochemical deintercalation of lithium caused a significant increase in the peak heights for all peaks. Since the trivalent manganese is a Jahn–Teller ion, its oxygen coordination is expected to be a distorted $Mn–O_6$ octahedron. The deintercalation of lithium causes the oxidation of Mn^{3+} to Mn^{4+}, which decreases the local structural disorder caused by the existence of the Jahn–Teller distorted octahedra. This accounts for the observed increase in intensity of the peaks. Besides the decrease in the distortion, oxidation of manganese also causes an increase in the regularity of the octahedra. The average oxidation state of the Mn ion is 3.6 for nominal $LiMn_{5/3}Cr_{1/3}O_4$, and 3.92 for $x = 0.53$. Thus, the existence of mixed $Mn^{3+}–O_6$ and $Mn^{4+}–O_6$ octahedra results in regular $Mn^{4+}–O_6$ octahedra, which also contribute to the increase in the FT.

The effect of chromium substitution on the FT of the Mn K-edge EXAFS of $Li(Mn_{2-y}Cr_y)O_4$ as a function of y was also examined for ($y = 0$, 1/9, 1/6 and 1/3). The result shows that both the Mn–O and Mn–M peaks increased with y. This suggests that chromium substitution leads to an increase in local order around the manganese.

Curve-fitting analysis of the EXAFS oscillations in wave-vector space leads to structural parameters relating to the manganese and oxygen atoms. For $y = 1/3$, the octahedral Mn–O distances for $x = 0$ and 0.53 were 1.91 and 1.91 Å, respectively. The deintercalation of lithium causes no significant change in the octahedral Mn–O distance. In contrast, the Mn–M distances for $x = 0$ and 0.53 were 2.89 and 2.86 Å, respectively. The Mn–M distance is directly related to the cell dimensions of the spinel structure. The observed shrinkage of the Mn–M distance, thus, suggests a shrinkage of the cell-size due to lithium deintercalation.

It is reported that the cycling performance of the battery is improved by the substitution of other metals (M = Cr, Ni, Co) for Mn in $LiMn_2O_4$ and that $Li(Mn, Co)_2O_4$ has a higher discharge capacity than other substituted spinels [4,5]. For the case of Cr, the substitution of the chromium for manganese helps stabilize the spinel structure and does not appear to contribute to charging in the 4 V region. On the other hand, a separate study has revealed that $Li(Mn, Co)_2O_4$ shows improvements not only in its cycling performance, but also in its discharge capacity, because cobalt contributes both to structure stabilization and the charging process in the 4 V region [18].

References

[1] M.M. Thackeray, A. de Kock, W.I.F. David, Mater. Res. Bull. 28 (1993) 1041.
[2] D. Guyomard, J.M. Tarascon, Solid State Ionics 69 (1994) 222.
[3] J.M. Tarascon, W.R. McKinnon, F. Coowar, T.N. Bowmer, G. Amatucci, D. Guyomard, J. Electrochem. Soc. 141 (1996) 1783.
[4] R. Bittihn, R. Herr, D. Hoge, J. Power Sources 43/44 (1993) 223.
[5] G. Li, H. Ikuta, T. Uchida, M. Wakihara, J. Electrochem. Soc. 143 (1996) 178.
[6] M. Wakihara, G. Li, H. Ikuta, in: M. Wakihara, O. Yamamoto (Eds.), Lithium Ion Batteries, Wiley, Tokyo, 1998, p. 26.
[7] D. Song, H. Ikuta, T. Uchida, M. Wakihara, Solid State Ionics 117 (1999) 151.
[8] N. Hayashi, H. Ikuta, M. Wakaihara, J. Electrochem. Soc. 146 (1999) 1351.
[9] B. Ammundsen, D.J. Jones, J. Roziere, J. Phys. Chem. B102 (1998) 7939.
[10] B. Ammundsen, M.S. Islam, D.J. Jones, J. Roziere, J. Power Sources 81/82 (1999) 505.
[11] I. Nakai, Y. Shiraishi, F. Nishikawa, Spectrochim. Acta B 54 (1999) 143.
[12] I. Nakai, K. Takahashi, Y. Shiraishi, T. Nakagome, F. Izu, I.Y. Ishii, F. Nishikawa, T. Konishi, J. Power Sources 68 (1997) 536.
[13] Y. Shiraishi, I. Nakai, T. Tsubata, T. Himeda, F. Nishikawa, J. Solid State Chem. 133 (1997) 587.
[14] I. Nakai, K. Takahashi, Y. Shiraishi, T. Nakagome, F. Nishikawa, J. Solid State Chem. 140 (1998) 145.
[15] I. Nakai, T. Nakagome, Electrochem. Solid State Lett. 1 (1998) 259.
[16] Rigaku EXAFS Analysis Software, REX2, Cat. No. 2612S211, Rigaku Co., 1996.
[17] A.L. Ankudinov, B. Ravel, J.J. Rehr, S.D. Conradson, Phys. Rev. B 58 (1998) 7565.
[18] Y. Terada, K. Yasaka, F. Nishikawa, T. Konishi, M. Yoshio, I. Nakai, J. Solid State Chem. 156 (2001) 286.